Revista Brasileira de Farmacognosia (2023) 33:736–746
https://doi.org/10.1007/s43450-023-00397-4

ORIGINAL ARTICLE

A Novel Caffeoylquinic Acid from *Lonicera japonica* Exerts Cytotoxic Activity by Blocking the YAP-CTGF Signaling Pathway in Hepatocellular Carcinoma

Wanying Shen[1,2,3,4] · Xiaofang Wei[1,2,3,4] · Yangfang Li[2,3,5] · Chenxiao Liu[2,3,5] · Lanlan Ge[2,3,5] · Jie Yao[2,3,5] · Xiaobin Zeng[2,3,5] · Xudong Tang[1,4]

Received: 4 October 2022 / Accepted: 4 April 2023 / Published online: 31 May 2023

Abstract

We have purified a novel caffeoylquinic acid named 3,4-di-*O*-caffeoylquinic acid isobutyl ester from the flower buds of *Lonicera japonica* Thunb., Caprifoliaceae. However, the biological function of 3,4-di-*O*-caffeoylquinic acid isobutyl ester is still unknown. Here, we found that 3,4-di-*O*-caffeoylquinic acid isobutyl ester effectively inhibited the proliferation and migration of hepatocellular carcinoma cells, and it displayed less toxicity to a normal liver cell line. Mechanistic studies showed that 3,4-di-*O*-caffeoylquinic acid isobutyl ester diminished the expression of YAP at the mRNA level. Overexpression of YAP significantly rescued HepG2 cells from the 3,4-di-*O*-caffeoylquinic acid isobutyl ester–induced suppression of proliferation and migration. Furthermore, the YAP downstream target gene CTGF was significantly repressed upon 3,4-di-*O*-caffeoylquinic acid isobutyl ester treatment, which was ameliorated by YAP overexpression. In addition, 3,4-di-*O*-caffeoylquinic acid isobutyl ester decreased the expression of β-catenin as well as CDK4/6. Collectively, 3,4-di-*O*-caffeoylquinic acid isobutyl ester exerts antihepatocellular carcinoma activity by inhibiting the YAP-CTGF pathway which controls the proliferation and migration of hepatocellular carcinoma cells. The Wnt/β-catenin pathway might be another pathway by which 3,4-di-*O*-caffeoylquinic acid isobutyl ester exerts antihepatocellular carcinoma activity. As a novel natural compound, 3,4-di-*O*-caffeoylquinic acid isobutyl ester might be a promising agent for hepatocellular carcinoma therapy.

Keywords New drug · Chinese herbal medicines · Primary liver cancers · *In vitro* · The Hippo signaling pathway · The Wnt signaling pathway

Introduction

Hepatocellular carcinoma (HCC), which accounts for the majority of primary liver cancers, is a malignant digestive system tumor (Singal et al. 2020). Hepatocellular carcinoma usually occurs in the context of oxidative stress and inflammation, caused by chronic hepatitis B or C virus (HBV or HCV), alcoholic and nonalcoholic steatohepatitis, and aflatoxin-mediated toxicity (Shariff et al. 2009; Petrick et al. 2020). Hepatocellular carcinoma has the sixth highest incidence rate (Villanueva 2019) and is the fourth largest cause of cancer-related death worldwide (Bray et al. 2018). At present, the first-line drugs sorafenib and lenvatinib as well as the second-line drug regorafenib

✉ Lanlan Ge
gelanlan@szhospital.com

✉ Jie Yao
yaojie@whu.edu.cn

✉ Xiaobin Zeng
zeng.xiaobin@szhospital.com

✉ Xudong Tang
tangxd@tsinghua-sz.org

[1] College of Pharmacy, Gansu University of Chinese Medicine, Lanzhou, China

[2] Center Lab of Longhua Branch and Department of Infectious Disease, Shenzhen People's Hospital The Second Clinical Medical College, Jinan University , Shenzhen, Guangdong, China

[3] The First Affiliated Hospital, Southern University of Science and Technology, Shenzhen, Guangdong, China

[4] Key Laboratory of Innovative Traditional Chinese Medicine and Natural Medicine, Research Institute of Tsinghua University, Shenzhen, Guangdong, China

[5] Centre Lab of Longhua Branch and Department of Infectious Disease, 2nd Clinical Medical College (Shenzhen People's Hospital) of Jinan University, Shenzhen, Guangdong, China

are being used for advanced HCC (Villanueva 2019). However, the survival benefit of sorafenib and regorafenib only obtained an additional 2–3 months of overall survival (Llovet et al. 2008) (Cheng et al. 2009). Lenvatinib was noninferior to sorafenib in overall survival in untreated advanced HCC (Kudo et al. 2018). In addition, many patients with liver cancer do not tolerate drug toxicity, and some patients may acquire adaptive drug resistance (Llovet et al. 2018; Yau et al. 2011). Therefore, there is an urgent need to develop less toxic and more effective potential drugs for HCC treatment.

The Hippo/YAP pathway, a cellular signal transduction pathway with high conservation, plays an important role in controlling organ size and tumorigenesis. Core components of the Hippo pathway include Mst1/2, Lats1/2, and yes-associated protein (YAP) which is the ultimate effector of the Hippo pathway. The phosphorylation of YAP at Ser127 leads to cytoplasmic retention of YAP and suppression of its transcriptional activity (Callus et al. 2006; Yu et al. 2012; Ma et al. 2019). YAP participates in signal transduction and regulates the transcription of genes including CYR61 and CTGF (Zhao et al. 2010; Wang et al. 2016). Increased expression of YAP has been detected in HCC (Cho et al. 2021). Moreover, high expression of YAP was positively correlated with the tumor volume of HCC (Wu et al. 2016). YAP is a potential therapeutic target in HCC development.

The Wnt/β-catenin pathway is a key molecular mechanism involved in embryonic development and tissue homeostasis (Krishnamurthy and Kurzrock 2018). Aberrant activation of the Wnt/β-catenin pathway is one of the important reasons for the occurrence and development of a variety of cancers (Zhang and Wang 2020). β-Catenin is the ultimate downstream effector of the canonical Wnt signaling pathway. Cytoplasmic retention and expression are tightly controlled by a multiprotein destruction complex composed of adenomatous polyposis coli (APC), AXIN, and glycogen synthase kinase-3β (GSK3β). This complex phosphorylates β-catenin at Ser37 and Thr41. The phosphorylation of β-catenin leads to its ubiquitination and proteasome-mediated degradation (Nong et al. 2021). β-Catenin regulates the expression of target oncogenes including c-MYC and CCND1 by combining with lymphoid enhancer/transcription factor (lef/tcf) (Katoh 2018). Aberrant β-catenin activation has been detected in HCC in both humans and rodents (Cassano et al. 2017). β-Catenin expression is inversely correlated with survival in HCC tumor tissues (Huo et al. 2021). Targeting β-catenin might be an effective strategy for anti-HCC therapy.

Chinese herbal medicines have long been applied in the clinic because of their advantages of low toxicity and targeting of multiple factors and pathways (Li et al. 2022). The flower bud of *Lonicera japonica* Thunb., Caprifoliaceae, is a traditional herbal medicine with various biological activities, including antihepatoma and anti-HBV activities (Ge et al. 2019). However, the underlying mechanism remains to be investigated. In our previous study, we purified a novel caffeoylquinic acid named 3,4-di-*O*-caffeoylquinic acid isobutyl ester (3,4-CQIE) from *L. japonica* flower buds. 3,4-CQIE (**1**) is a pale-yellow amorphous powder. The formula of 3,4-CQIE is $C_{29}H_{31}O_{12}$ and its molecular weight is 571.08. Preliminary studies showed that it had potential anti-HCC activity. However, its molecular mechanisms need to be further explored. In the present study, we further investigated the anti-HCC activity of 3,4-CQIE and the underlying molecular mechanism.

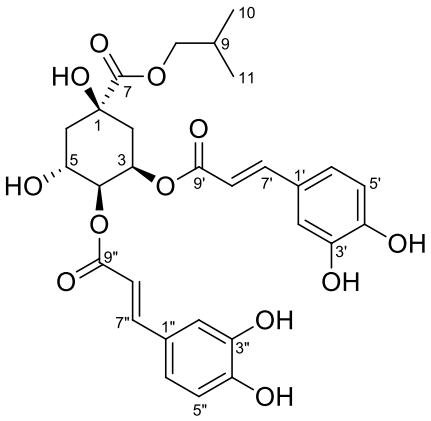

1

Materials and Methods

Antibodies

Antibodies, including CDK6 (A0705), CDK4 (A11136), β-actin (AC004), and CTGF (A11067), were purchased from ABclonal; β-catenin (8480 T), CCND1 (2978S), TAZ (72804), and YAP (14074S) were purchased from Cell Signaling Technology. The second HRP-linked antibodies were anti-mouse IgG (7076S) and anti-rabbit IgG (7074S), which were purchased from Cell Signaling Technology. Alexa Fluor 594–conjugated donkey anti-rabbit IgG (H + L) (Invitrogen, R97402), Alexa Fluor 488–conjugated donkey anti-mouse IgG (H + L) (Invitrogen, R37118), and Alexa Fluor 488–conjugated donkey anti-rabbit IgG (H + L) (Invitrogen, R37118) were used as secondary antibodies for the immunofluorescence assay.

Reagents

Cell Counting Kit-8 (Apexbio, K1018) was purchased from APE × BIO, and twenty-four-well transwell plates (6.5 mm) with 8 μM polycarbonate membrane inserts (3422) were obtained from Corning Incorporated. Trypsin solution

(25200072) and Opti-MEM® I (31985062) were purchased from Gibco (Guangzhou, China); a Lipofectamine® 3000 Transfection Kit (L3000-001) was purchased from Thermo Fisher (Guangzhou, China). Dimethyl sulfoxide (67-68-5) was purchased from BBI Life Sciences (Beijing, China); 4′6-diamidino-2-phenylindole (C0065), glue preparation (A1010), and thiol-reducing agent (M8210) were purchased from Solarbio (Beijing, China). A protein marker (22AB1001) was purchased from Mei5 Biotechnology Co., Ltd. (Beijing, China). Antifade mounting solution (P0186) and primary antibody diluent (P0023A) were purchased from Beyotime (Beijing, China). A PVDF membrane (IPVH00010) was purchased from Millipore (Beijing, China); a TIANprep Mini Plasmid Kit (DP103-03) was purchased from Tiangen (Beijing, China); and an EASYspin organization/cell RNA Rapid extraction kit (RN07) was purchased from Adelaide (Beijing, China).

Isolation of 3,4-CQIE

3,4-CQIE (**1**) was isolated from *L. japonica* flower buds, which were collected in May 2017 from Pingyi County, Linyi City, Shandong Province. The plants were identified by Dr. XB Zeng of Shenzhen People's Hospital, and a voucher specimen (No. 20170930) was deposited at the Center Lab of Longhua Branch, Shenzhen People's Hospital, Second Clinical Medical College of Jinan University, Shenzhen, China. The extraction and isolation procedure of 3,4-CQIE was described in detail in our previous patent (application number CN202111148950.5).

Extraction and isolation of 3,4-CQIE: The air-dried and powdered flowers (6.5 kg) of *L. japonica* were percolated with 75% (v/v) ethanol at room temperature to afford a crude extract (1.5 kg), which was then suspended in water and successively partitioned with cyclohexane, ethyl acetate, and *n*-butanol to yield crude extracts. The *n*-butanol extract (180 g) was subjected to silica gel column chromatography eluting with CH_2Cl_2-MeOH (100:0 to 0:100, v/v) to afford forty major fractions (LB1–LB40). LB5 (3 g) was then re-subjected to Sephadex LH-20 column chromatography (CH_2Cl_2-MeOH, 3:7, v/v) to afford twenty subfractions (LB5-1–LB5-20). LB5-13 was re-subjected to Sephadex LH-20 column chromatography eluting with CH_2Cl_2-MeOH (1:1, v/v) to afford fifteen subfractions (LB5-13–1−LB5-13-15), and LB5-13-14 was subsequently purified by preparative HPLC (Cosmosil 5C18-MS-II, 5 μm, 20 × 250 mm, 8 ml/min, 254 nm, MeOH–H_2O, 54:46, v/v) to obtain 3,4-di-*O*-caffeoylquinic acid isobutyl ester (26.6 mg).

HPLC of 3,4-CQIE

High-performance liquid chromatography (HPLC) analysis was carried out on an Essentia LC-16 HPLC system (Shimadzu, Tokyo, Japan) equipped with a diode-array detector. All separations were performed using a YMC-Pack ODS-A column (4.6 mm × 250 mm, 5 μm) with a flow rate of 1 ml/min. The mobile phase was eluted with 50% methanol in water. The injection volume of the test sample was set at 10 μl each time, and the UV spectra were recorded at 330 nm. The isolation of 3,4-CQIE in this study has been patented in China (application number CN202111148950.5).

Spectral Equipment

Nuclear magnetic resonance (NMR) spectra were recorded on a Bruker DPX-400 (1H NMR, 400 MHz; ^{13}C NMR, 100 MHz) spectrometer, with tetramethylsilane (TMS) as the internal standard. Unless otherwise specified, chemical shifts (δ) were quoted in ppm with reference to the residual solvent signal (DMSO-d6: δ_H 2.50 ppm, δ_C 39.52 ppm). Negative-ion HR-ESI-TOF-MS data were measured using a Bruker microTOF-QII mass spectrometer (Bruker, Karlsruhe, Germany).

Cell Culture

Human hepatocellular carcinoma (HCC) cell lines HepG2 and Huh7 were purchased from the American Type Culture Collection (ATCC, Manassas, VA, USA). Human normal liver epithelial THLE-3 cells were purchased from the Cell Bank of Chinese Academy. All cells were cultured in DMEM (Vivacell, C3113-0500) medium, supplemented with 10% fetal bovine serum (FBS, Hyclone, Logan, UT, USA, 10100147C), 100 U/ml penicillin, and 100 mg/ml streptomycin (Beyotime, 10378016). All cells were cultured at 37 °C in a 5% CO_2 incubator.

Cell Viability

Cell viability was detected by CCK-8 assays. Briefly, cells (5×10^3 cells per well for HepG2 and THLE-3 and 2.5×10^3 cells per well for Huh7) were seeded in 96-well plates and cultured for 24 h, followed by exposure to various concentrations of 3,4-CQIE (0, 40, 60, 80, 100, 120, and 140 μM) for 24 and 48 h, respectively. CCK8 reagent, 10%, was added to each well and incubated for another 2 ~ 3 h. Optical density values at 450 nm were detected using a microplate reader.

Wound-Healing Assay

The first step in the scratch wound-healing assay was to place the culture insert into 24-well plates, and 70 μl suspension, including 1×10^5 cells, was placed in the culture insert for 12 h to form a confluent monolayer. The culture inserts were then removed.

The cells were washed once with PBS to remove cell debris and cultured with DMEM containing 5% serum with 3,4-CQIE (0, 100, and 120 μM) for HepG2 cells, or DMEM without serum with 3,4-CQIE (0, 100, and 120 μM) for Huh7 cells. The migration distances of the cells were observed under a light microscope when the cells were cultured at 37 °C for 0, 24, and 48 h.

Western Blot Assay

HepG2 and Huh7 cells were cultured on 12-well plates and treated with the indicated concentration of 3,4-CQIE for 48 h after adhesion. Whole cell lysates were collected and boiled in SDS lysis buffer (0.5 M Tris-HCl, pH 6.8, 2% SDS, 10% glycerol, and 0.1% bromophenol blue) at 95 °C for 15 min; 10% SDS-PAGE was performed and then transferred to a PVDF membrane (0.45 μM). The imprints were blocked in blocking buffer (skim milk in TBST) for 1 h at room temperature and then incubated with primary antibodies specific for β-actin (1:1000), CTGF (1:1000), TAZ (1:1000), YAP (1:1000), CDK6 (1:1000), CDK4 (1:1000), β-catenin (1:1000), and CCND1 (1:1000), after incubation with primary antibody for 1 h. The membranes were washed three times in tris-buffered saline containing 0.1% Tween-20 and incubated with the secondary antibodies anti-mouse IgG (1:5000) or anti-rabbit IgG (1:5000), then washed three times in tris-buffered saline containing 0.1% Tween-20 and Exposure development by ECL (Pierce Biotechnology, Rockford, IL, USA). Gels of western blot are one representative of three independent experiments. Quantitative analysis of western blot is presented as the mean ± SD of three independent experiments.

RT-qPCR

Total RNA was extracted using an RNA Rapid extraction kit (Aidlab, RN07) according to the manufacturer's protocol. cDNA was prepared with a reverse transcription kit (Vazyme, R211-02) using a Thermal Cycler (Bio-Rad Laboratories). The following cycling parameters were used: 1 cycle of 25 °C for 5 min, 50 °C for 15 min, and 85 °C for 2 min. RT-qPCR was performed using the One-Step SYBR PrimeScript Plus RT-PCR kit (Vazyme, Q711-02-AA). PCR primers were custom synthesized by Guangzhou IGE Technology (Guangzhou, China). Briefly, the primers, qPCR mix, and cDNA templates were mixed for the PCRs. RT-qPCR analysis was performed in a LightCycler® 480 Real-Time PCR System (Roche, Switzerland). The relative mRNA expression levels of the target genes were standardized with the housekeeping gene β-actin, the value of which was set as 100%. All of the reactions were run in triplicate, and the data were analyzed according to the comparative Ct (2-ddCt) method. All primers used in this study are listed in Table 1.

Immunofluorescence Assay

Cells were grown on coverslips. After the cells were treated with 3,4-CQIE, the cell culture was discarded, and the coverslips were fixed with 4% paraformaldehyde at room temperature to fix for 10 min and then washed with phosphate-buffered saline three times. The coverslips were then incubated with staining buffer (1% BSA and 0.1% Triton in PBS) for 10 min and washed with PBS three times. The coverslips were incubated with primary antibodies for YAP (1:100) and CTGF (1:100), and incubated with secondary antibodies for Alexa Fluor 594 (1:1000) or Alexa Fluor 488(1:1000) in the dark for 1 h. Finally, the coverslips were stained with 0.5 μg/ml DAPI for 10 min and visualized using a Leica TCS SP8 confocal microscope (Leica, Germany).

Transient Transfection

For transient transfection, HepG2 cells were seeded in six-well plates or twenty-well plates. The GFP-YAP and control plasmids were transfected into a HepG2 cell using Lipofectamine® 3000 Transfection Kit reagent following the manufacturer's protocol. Western blotting assays were performed to detect transfection efficiency after 48 h. The transfected cells were then used for CCK8 and a scratch wound-healing assay after transfection for 24 h.

Statistical Analysis

The experimental data are expressed as mean ± standard deviation ($x \pm s$). Comparisons between treatments were

Table 1 Information of primer

Assay	Gene names	Forward (5′–3′)	Reverse (5′–3′)
RT-PCR	β-Actin	CAGCACAATGAAGATCAAGA	GATCCACATCTGCTGGAAG
	YAP	TCTTCCTGATGGATGGGAAC	TTGGGTCTAGCCAAGAGGTG
	CTGF	CTTGTCTGATCGTTCAAAGC	CAATCTGTTTTGACGGACTG
	CDK4	ACAGTTCGTGAGGTGGCTTT	TACCTTGATCTCCCGGTCAG
	CDK6	GAGGCACCTGGAGACCTTC	TGGTTTCTCTGTCTGTTCGTG
	CCND1	TGGTGAACAAGCTCAAGTGG	CTCTGGCATTTTGGAGAGGA
	β-Catenin	GGAAGAGTCCGGAGGAGATG	CTGGCTGTCAGGTTTGATCC

performed using ANOVA, followed by Tukey's test. Statistical significance was set at $p < 0.05$, and software such as Graphpad, Adobe Photoshop, and ImageJ is used for graphing.

Results and Discussion

Structural Elucidation

Compound **1** was obtained as a pale-yellow amorphous powder. The negative deprotonated molecule $[M-H]^-$ in its HR-ESI-MS data at *m/z* 571.1667 $[M-H]^-$ (calcd.for $C_{29}H_{31}O_{12}$, 571.0806) together with the ^{13}C NMR spectral data suggested a molecular formula of $C_{29}H_{32}O_{12}$. The 1D and 2D NMR data of **1** resembled those of 3,4-di-*O*-caffeoylquinic acid isobutyl ester, and the major difference was the replacement of a methyl group at C-8 (δ_C 52.5) in 3,4-di-*O*-caffeoylquinic acid methyl ester by an isobutyl motif (δ_C 70.4, C-8; δ_C 27.2, C-9; δ_C 18.9, C-10; δ_C 18.8, C-11) at the same position in **1** (Ge et al. 2018), as supported by the HMBC correlations from H_3-10 (δ_H 0.85)/H_3-11 (δ_H 0.82) to C-8. The planar structure of **1** was further confirmed with the aid of the 2D NMR spectroscopic analysis. Thus, compound **1** was assigned to be 3,4-di-*O*-caffeoylquinic acid isobutyl ester (Supplementary data; Figure S1-S8).

Inhibition of Proliferation

To determine the effect of 3,4-CQIE on cell proliferation, the cell viabilities of one normal liver epithelial cell line (THLE-3) and two HCC cell lines (HepG2 and Huh7) were measured via CCK8 assays. The results showed that 3,4-CQIE significantly reduced the viability of HepG2 (Fig. 1A, E) and Huh7 (Fig. 1B, F) cells. At 24 h postincubation, the half maximal inhibitory concentration (IC_{50}) values of 3,4-CQIE against THLE-3, HepG2, and Huh7 cells were 182.96 ± 6.07, 101.17 ± 3.75, and 110.89 ± 1.49 μM, respectively (Fig. 1C, D). At 48 h postincubation, their IC_{50} values were 156.11 ± 0.88, 86.27 ± 3.22, and 92.31 ± 0.21 μM, respectively (Fig. 1G, H). Based on IC_{50} calculations, 3,4-CQIE had a better antiproliferative effect on HCC cells (Fig. 1D, H). The results demonstrated that 3,4-CQIE had a strong antiproliferative effect on HCC cells and less toxicity to normal cells. At 24 h postincubation, the half maximal inhibitory concentration (IC_{50}) values of lenvatinib, an emerging first-line treatment for unresectable HCC, against HepG2 (Fig. 1I), Huh7 (Fig. 1J), and THLE-3 (Fig. 1K) cells were 42.90 ± 1.16, 41.64 ± 0.08, and 62.50 ± 2.84 μM, respectively. At 48 h postincubation, their IC50 values were 42.65 ± 0.40, 37.16 ± 0.49, and 49.55 ± 1.78 μM, respectively (Fig. 1L–P).

Inhibition of Migration

Increased migratory ability is one of the most prominent features of HCC cells (Weiler et al. 2020). To determine whether 3,4-CQIE affects cell migration, we conducted a wound-healing assay and discovered that the gaps between the cells were larger with 3,4-CQIE treatment than in the control group (Fig. 2A–D). Altogether, these data imply that 3,4-CQIE suppresses HCC cell migration.

Inhibition of YAP

To further explore the molecular mechanism of 3,4-CQIE against HCC, we examined the expression of key proteins of the Hippo pathway, including YAP, TAZ, and CTGF. The results showed that YAP and CTGF showed a downwards trend with increasing 3,4-CQIE concentrations (Fig. 3A, B). Therefore, we further carried out an immunofluorescence assay to explore the nuclear localization of YAP upon 3,4-CQIE treatment. The results showed an overall decrease in YAP staining intensity in 3,4-CQIE (120 μM)-treated HepG2 cells (Fig. 3C). In addition, the RT-PCR experiment showed that the mRNA level of YAP was decreased after 3,4-CQIE treatment (Fig. 3D). Moreover, the proteasome inhibitor MG132 could not rescue HCC cells from 3,4-CQIE-induced YAP degradation (Fig. 3E), indicating that YAP might be downregulated by 3,4-CQIE treatment at the mRNA level.

Overexpression of YAP

To further confirm the effect of YAP in HCC cells and elucidate how 3,4-CQIE regulates the proliferation and migration of HCC cells, we performed overexpression experiments by transfecting HepG2 cells with GFP-YAP plasmid and treating them with 3,4-CQIE. We first performed a western blot assay to confirm that cells transfected with the YAP plasmid had stronger expression of YAP than cells transfected with an empty vector (Fig. 4A). To detect the effect of YAP on 3,4-CQIE-induced proliferation arrest, we performed a CCK8 assay. The results showed that overexpression of YAP rescued the 3,4-CQIE-induced decrease in cell viability in HepG2 cells (Fig. 4B). The results suggested that YAP was involved in the anti-growth effect of 3,4-CQIE. Subsequently, wound-healing assays were conducted to assess the role of YAP in 3,4-CQIE-induced migration suppression. The results demonstrated that YAP overexpression significantly reduced the 3,4-CQIE-induced suppression of migration in HepG2 cells (Fig. 4C, D). Collectively, YAP plays a critical role in cell proliferation and migration in response to 3,4-CQIE.

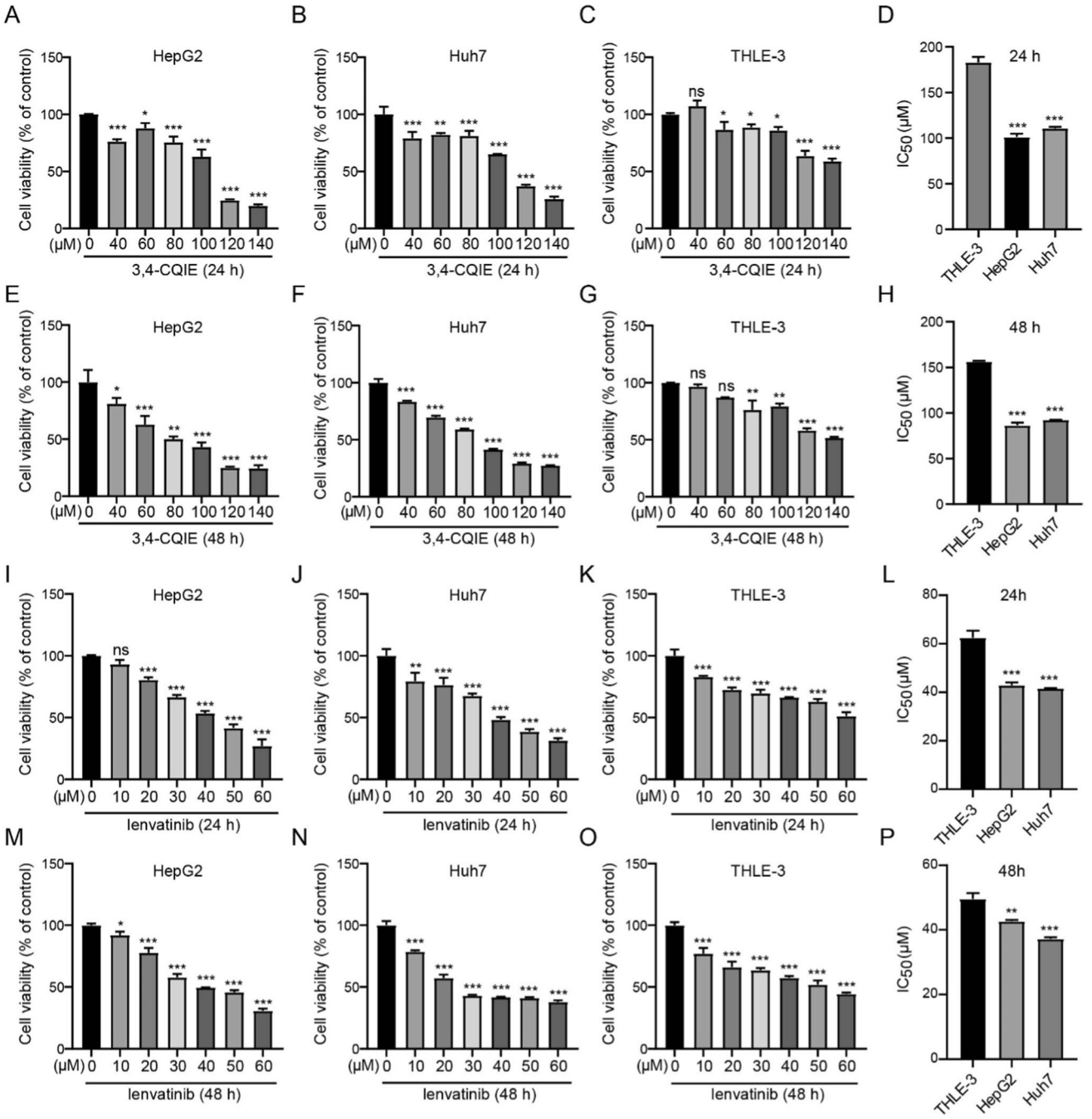

Fig. 1 3,4-CQIE (**1**) inhibits HCC cell growth. **A** and **E** HepG2 cells were exposed to 3,4-CQIE at the indicated doses for 24 or 48 h, and the dose-escalation effects of 3,4-CQIE were assessed by CCK8 assay. **B** and **F** Huh7 cells were exposed to 3,4-CQIE at the indicated doses for 24 or 48 h, and the dose-escalation effects of 3,4-CQIE were assessed by CCK8 assay. **C** and **G** THLE-3 cells were exposed to 3,4-CQIE at the indicated doses for 24 or 48 h, and the dose-escalation effects of 3,4-CQIE were assessed by CCK8 assay. **D** and **H** The inhibitory intensities of 3,4-CQIE were expressed as IC_{50} for 24 and 48 h. **I** and **M** HepG2 cells were exposed to lenvatinib at the indicated doses for 24 or 48 h, and the dose-escalation effects of lenvatinib were assessed by CCK8 assay. **J** and **N** Huh7 cells were exposed to lenvatinib at the indicated doses for 24 or 48 h, and the dose-escalation effects of lenvatinib were assessed by CCK8 assay. **K** and **O** THLE-3 cells were exposed to lenvatinib at the indicated doses for 24 or 48 h, and the dose-escalation effects of lenvatinib were assessed by CCK8 assay. **L** and **P** The inhibitory intensities of lenvatinib were expressed as IC_{50} for 24 and 48 h. Data are representative of three experiments with similar results. means ± SD, $*p < 0.05$, $**p < 0.01$, $***p < 0.001$ compared with the control group

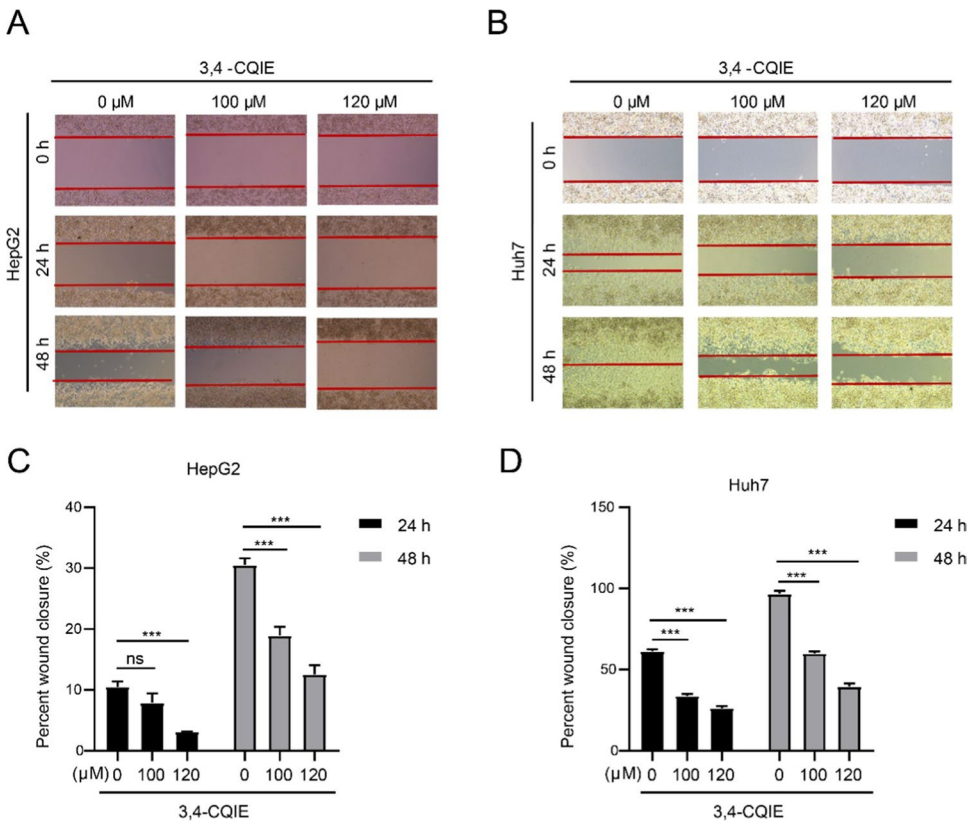

Fig. 2 3,4-CQIE (**1**) suppresses the migration of HCC cells. **A**, **B** HepG2 (**A**) and Huh7 (**B**) cells were seeded in 24-well plates with 3,4-CQIE at the indicated doses for 48 h. Cell migration was estimated by wound-healing assay. **C**, **D** Relative areas of HepG2 (**C**) and Huh7 (**D**) cells were calculated using ImageJ software. Data are representative of three experiments with similar results. Means ± SD, $^{***}p < 0.001$ compared with the control group

Inhibition of the YAP/CTGF Pathway

Acting as a transcription factor, YAP increases the expression of the target oncogene CTGF. Since 3,4-CQIE can significantly inhibit the expression of YAP, we wondered whether 3,4-CQIE might also regulate CTGF. RT-PCR was performed, and the results showed that 3,4-CQIE treatment significantly inhibited the mRNA levels of CTGF (Fig. 5A). Immunofluorescence assays then showed that YAP overexpression rescued the 3,4-CQIE-induced CTGF decrease (Fig. 5B). The results suggested that 3,4-CQIE repressed the expression of CTGF by inhibiting the expression of YAP.

Inhibition of β-Catenin

YAP overexpression failed to fully restore the 3,4-CQIE-induced decrease in cell viability, suggesting that the anti-HCC effect of 3,4-CQIE may have other mechanisms. The Wnt pathway plays an important role in HCC progression. β-Catenin is the core component of the Wnt pathway. CCND1 is the downstream target of β-catenin. CCND1 has been reported to activate cyclin-dependent kinases (CDK4/6), leading to phosphorylation of retinoblastoma (Rb) and resulting in promotion of cell cycle progression (Weinberg 1995). Here, we explored whether 3,4-CQIE treatment could affect the Wnt pathway. The results showed that 3,4-CQIE markedly reduced the expression of β-catenin and its downstream target gene CCND1 as well as CDK4/6 in a concentration-dependent manner (Fig. 6A–F). Moreover, 3,4-CQIE repressed the mRNA levels of β-catenin, CCND1, and CDK4/6 (Fig. 6G–J) in a concentration-dependent manner. Collectively, another way for 3,4-CQIE to exert its anti-HCC effect may be dependent on inhibiting β-catenin expression as well as cell cycle–related proteins.

Discussion

Accumulating evidence indicates that the overexpression of YAP plays a critical role in the proliferation and migration of HCC cells (Cho et al. 2021). Therefore, we examined the mRNA and protein levels of YAP in 3,4-CQIE-treated HepG2 cells and found that YAP expression was downregulated by 3,4-CQIE treatment at the mRNA level but not at the protein level. We also found that 3,4-CQIE decreased the transcription of CTGF, which has been reported as a YAP downstream target gene. In our study, YAP overexpression restored the 3,4-CQIE-induced repression of CTGF. CTGF has been reported to promote the proliferation and migration of HCC cells. These results suggest that 3,4-CQIE might exert anti-HCC activity by inhibiting the YAP-CTGF pathway.

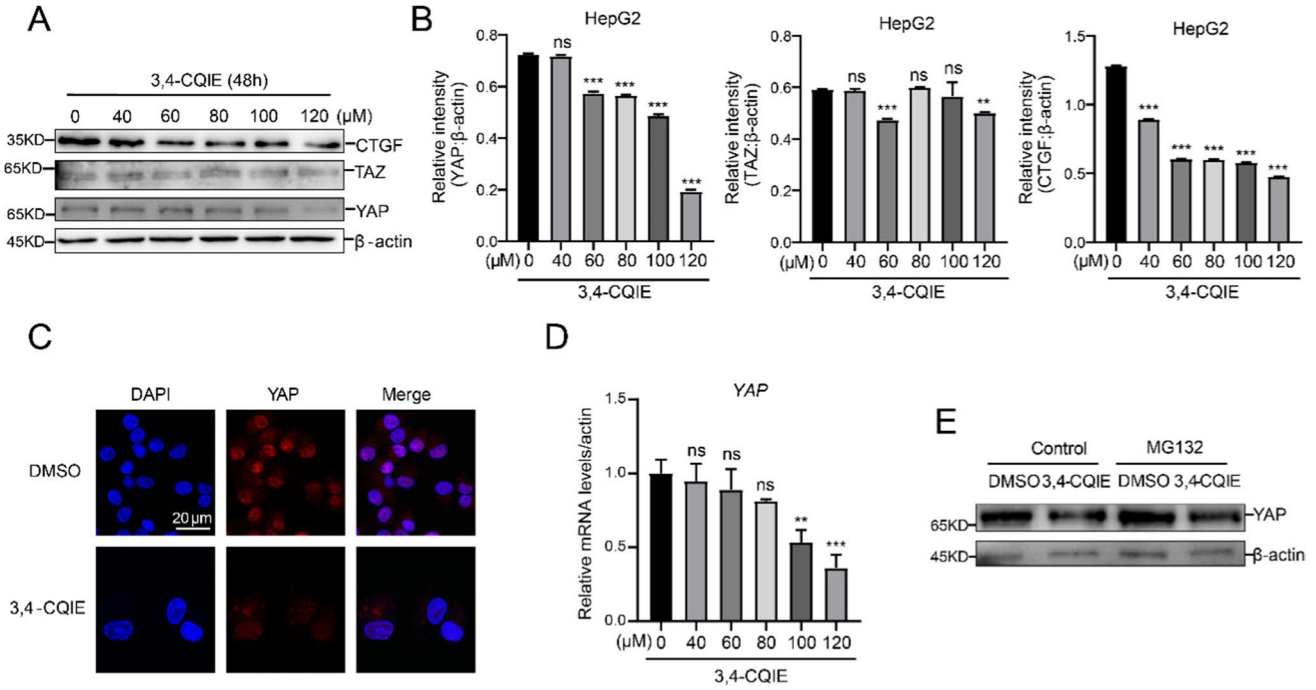

Fig. 3 3,4-CQIE (**1**) decreases the expression of YAP. **A** HepG2 cells were exposed to 3,4-CQIE at the indicated doses for 48 h, and cell lysates were immunoblotted with the indicated antibodies. β-Actin was used as an internal control in western blotting. **B** ImageJ statistical analysis was performed simultaneously. **C** HepG2 cells were exposed to the indicated dose of 3,4-CQIE for 48 h, and the expression of YAP was examined by confocal microscopy. The scale bars represent 20 μm. **D** HepG2 cells were treated with DMSO or 3,4-CQIE (40, 60, 80, 100, and 120 μM) for 48 h. The mRNA level of YAP was assessed by RT-PCR. **E** HepG2 cells were pretreated with DMSO alone, 3,4-CQIE (120 μM) alone for 48 h, or DMSO or 3,4-CQIE for 44 h, followed by the addition of 5 μM MG132 for an additional 4 h. Cell lysates were harvested and subjected to western blotting with anti-YAP antibodies. Means ± SD, $^{**}p < 0.01$, $^{***}p < 0.001$ compared with the control group

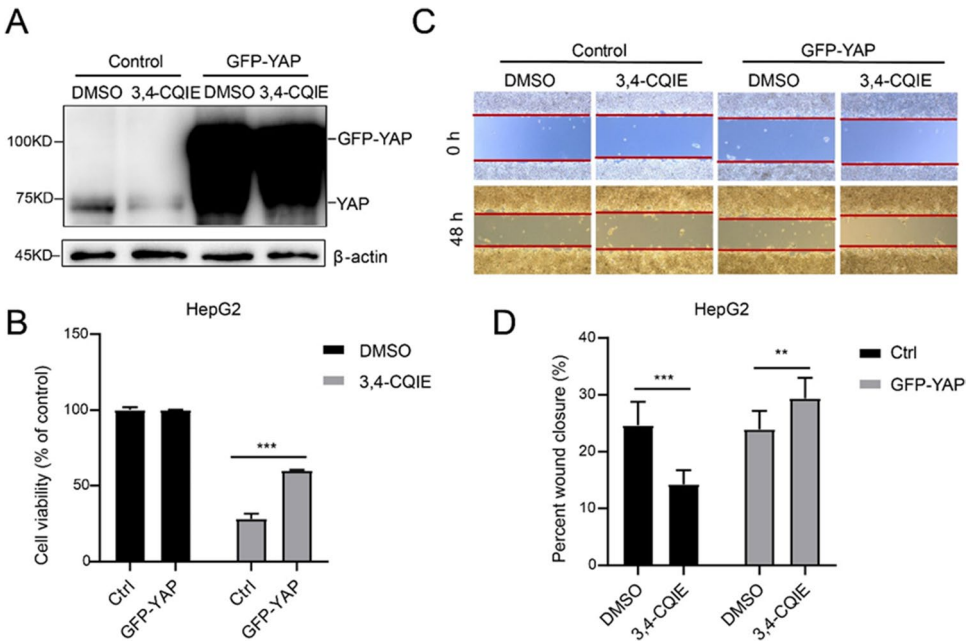

Fig. 4 3,4-CQIE (**1**) regulates proliferation and migration through YAP. **A** HepG2 cells were transfected with YAP for 24 h, and then treated with 3,4-CQIE (120 μM) for 48 h. GFP-YAP plasmid transfection increased YAP expression, as detected by western blotting assays. **B** HepG2 cells were transfected with YAP for 24 h and then treated with 3,4-CQIE (120 μM) for 48 h to detect cell viability. **C** HepG2 cells were transfected with control vector and YAP plasmid and then treated with 3,4-CQIE (120 μM) for 48 h. Cells were subjected to a scratch wound-healing assay. **D** Relative areas of HepG2 cells were calculated using GraphPad software. Data are representative of three experiments with similar results. Means ± SD, $^{**}p < 0.01$, $^{***}p < 0.001$ compared with the control group

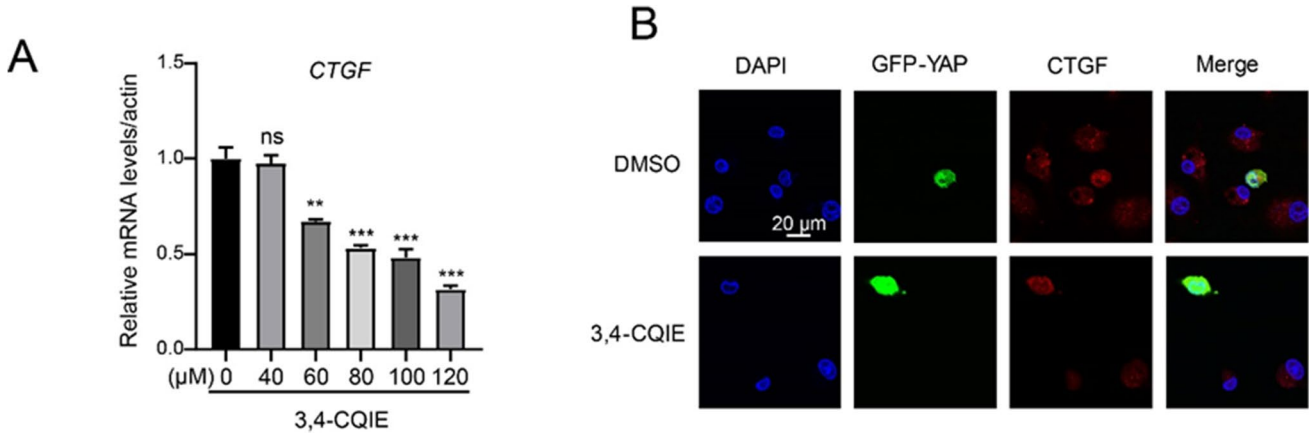

Fig. 5 3,4-CQIE (**1**) regulates proliferation and migration through YAP. **A** HepG2 cell lysates treated with the indicated concentrations of 3,4-CQIE were subjected to a quantitative RT-PCR assay to measure the mRNA level of CTGF. **B** HepG2 cells transiently transfected with GFP-YAP were treated with 120 μM 3,4-CQIE for 48 h and stained with antibodies against CTGF. Scale bar: 20 μm. Data are representative of three experiments with similar results. Means ± SD, $^{**}p < 0.01$, $^{***}p < 0.001$ compared with the control group

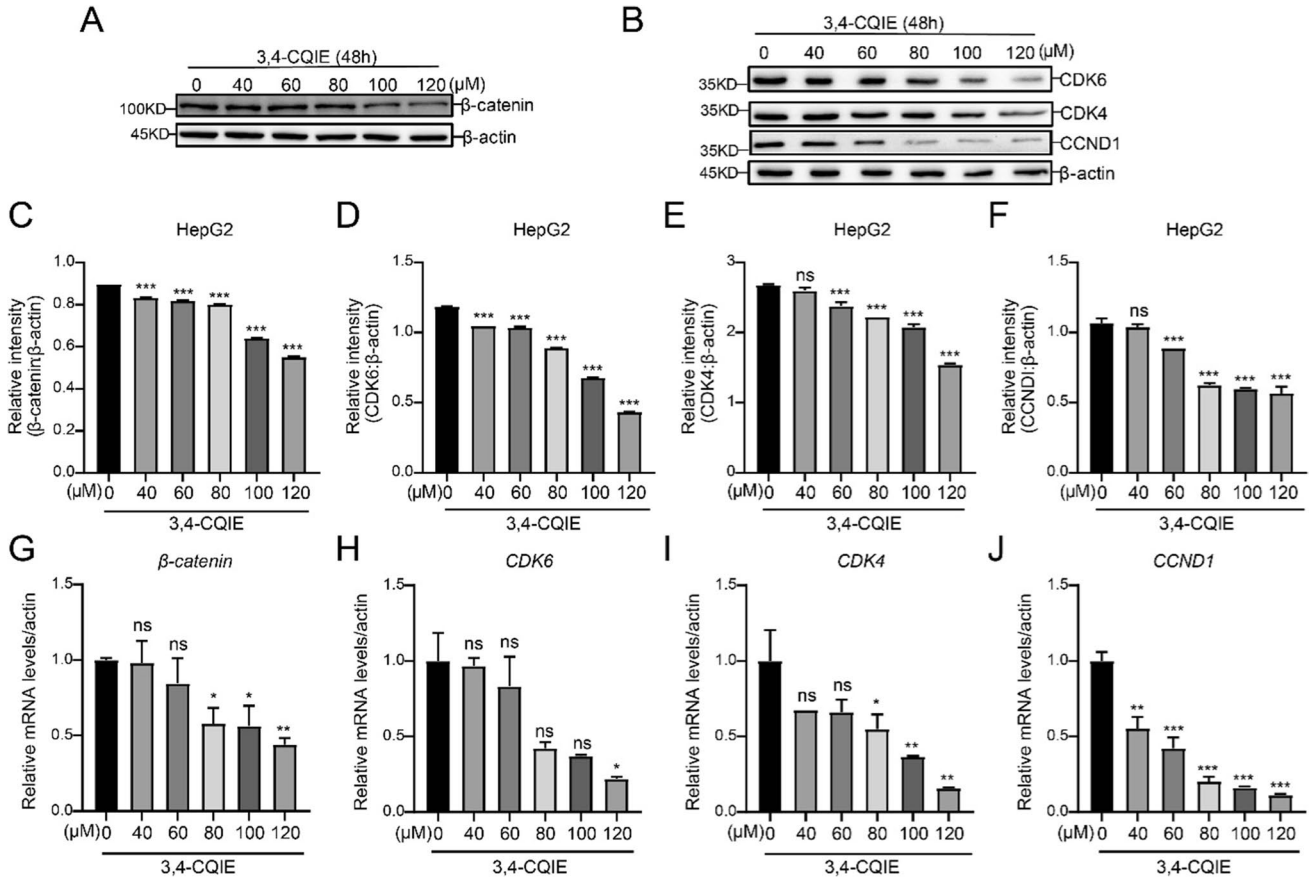

Fig. 6 3,4-CQIE (**1**) inhibits β-Catenin expression as well as cell cycle–related proteins. **A** and **B** HepG2 cells were exposed to 3,4-CQIE at the indicated doses for 48 h, and cell lysates were immunoblotted with the indicated antibodies. β-Actin was used as an internal control in western blotting. **C**–**F** ImageJ statistical analysis of the protein levels of β-Catenin (**C**), CDK6 (**D**), CDK4 (**E**), and CCND1 (**F**). **G**–**J** HepG2 cells were treated with DMSO or 3,4-CQIE (40, 60, 80, 100, and 120 μM) for 48 h. The mRNA levels of β-Catenin (**G**), CDK6 (**H**), CDK4 (**I**), and CCND1 (**J**) were assessed by RT−PCR. Data are representative of three experiments with similar results. Means ± SD, $^{*}p < 0.05$, $^{**}p < 0.01$, $^{***}p < 0.001$ compared with the control group

YAP overexpression could not completely restore the 3,4-CQIE-induced decrease in cell viability, indicating that the anti-HCC effect of 3,4-CQIE could also be exerted indirectly through other proteins. The Wnt/β-catenin pathway plays an important role in HCC progression (Perugorria et al. 2019). In addition, there are β-catenin-acquired mutations in approximately 20 to 40% of HCC patients, and FDA-approved drugs targeting β-catenin have not yet been used in the clinic (Rao et al. 2017). In the present study, we found that 3,4-CQIE could induce β-catenin degradation and repress the expression of CCND1, which has been reported as one of the β-catenin downstream target genes. Collectively, on the one hand, 3,4-CQIE suppressed the proliferation and migration of HCC cells by inhibiting the Hippo/YAP pathway; on the other hand, 3,4-CQIE might induce cell cycle arrest in HCC cells by inhibiting the Wnt/β-catenin pathway. These results suggested that both the Hippo/YAP and Wnt/β-catenin pathways were most likely involved in the 3,4-CQIE-induced suppression of HCC cells and implied that 3,4-CQIE might be a promising agent for HCC therapy.

Conclusion

3,4-CQIE is a novel natural caffeoylquinic acid purified from *L. japonica* flower buds. In this study, we found that 3,4-CQIE could significantly inhibit the viability and migration of HCC cells but had much less effect on normal liver cells. Further research revealed that 3,4-CQIE treatment led to a decrease in YAP and its target gene CTGF. In addition, 3,4-CQIE decreased the expression of β-catenin protein and its downstream gene CCND1, which promoted cell cycle progression. Collectively, we identified that a caffeoylquinic acid, 3,4-CQIE, suppressed HCC cell growth *in vitro* by inhibiting YAP and β-Catenin mRNA expression. Notably, 3,4-CQIE might be valuable as a potential drug for HCC therapy.

Patents

The isolation of 3,4-CQIE in this paper has been patented in China (application number CN202111148950.5.).

Supplementary Information The online version contains supplementary material available at https://doi.org/10.1007/s43450-023-00397-4.

Author Contribution Conceptualization: YJ, TXD, and ZXB; methodology: YJ and GLL; software: SWY; validation: SWY; formal analysis: WXF; investigation: TXD and ZXB; resources: LYF; data curation: SWY; writing—original draft preparation: YJ; writing and editing: YJ; visualization: SWY; supervision: LCX; project administration: YJ, TXD, and ZXB; funding acquisition: YJ and GLL.

Funding This work was supported by grants from National Natural Science Foundation of China (81903760, 82204682), Guangdong Basic and Applied Basic Research (2021A1515110841), Shenzhen Science and Technology Program (JCYJ20210324113003007, JCYJ20190806151816859).

Data Availability The data presented in this study are available on request from the corresponding author.

Declarations

Ethical Approval Not applicable.

Conflict of Interest The authors declare no competing interests.

Informed Consent Not applicable.

References

Bray F, Ferlay J, Soerjomataram I, Siegel RL, Torre LA, Jemal A (2018) Global cancer statistics 2018: GLOBOCAN estimates of incidence and mortality worldwide for 36 cancers in 185 countries. CA Cancer J Clin 68:394–424. https://doi.org/10.3322/caac.21492

Callus BA, Verhagen AM, Vaux DL (2006) Association of mammalian sterile twenty kinases, Mst1 and Mst2, with hSalvador via *C*-terminal coiled-coil domains, leads to its stabilization and phosphorylation. FEBS J 273:4264–4276. https://doi.org/10.1111/j.1742-4658.2006.05427.x

Cassano M, Offner S, Planet E, Piersigilli A, Jang SM, Henry H, Trono D (2017) Polyphenic trait promotes liver cancer in a model of epigenetic instability in mice. Hepatology 66:235–251. https://doi.org/10.1002/hep.29182

Cheng AL, Kang YK, Chen Z, Tsao CJ, Qin S, Kim JS, Guan Z (2009) Efficacy and safety of sorafenib in patients in the Asia-Pacific region with advanced hepatocellular carcinoma: a phase III randomised, double-blind, placebo-controlled trial. Lancet Oncol 10:25–34. https://doi.org/10.1016/S1470-2045(08)70285-7

Cho K, Ro SW, Lee HW, Moon H, Han S, Kim HR, Kim DY (2021) YAP/TAZ suppress drug penetration into hepatocellular carcinoma through stromal activation. Hepatology 74:2605–2621. https://doi.org/10.1002/hep.32000

Ge L, Wan H, Tang S, Chen H, Li J, Zhang K, Zeng X (2018) Novel caffeoylquinic acid derivatives from *Lonicera japonica* Thunb. flower buds exert pronounced anti-HBV activities. RSC Adv 8:35374–35385. https://doi.org/10.1039/c8ra07549b

Ge L, Xiao L, Wan H, Li J, Lv K, Peng S, Zeng X (2019) Chemical constituents from *Lonicera japonica* flower buds and their anti-hepatoma and anti-HBV activities. Bioorg Chem 92:103198. https://doi.org/10.1016/j.bioorg.2019.103198

Huo J, Wu L, Zang Y (2021) Development and validation of a CTNNB1-associated metabolic prognostic model for hepatocellular

carcinoma. J Cell Mol Med 25:1151–1165. https://doi.org/10.1111/jcmm.16181
Katoh M (2018) Multilayered prevention and treatment of chronic inflammation, organ fibrosis and cancer associated with canonical WNT/betacatenin signaling activation (Review). Int J Mol Med 42:713–725. https://doi.org/10.3892/ijmm.2018.3689
Krishnamurthy N, Kurzrock R (2018) Targeting the Wnt/beta-catenin pathway in cancer: update on effectors and inhibitors. Cancer Treat Rev 62:50–60. https://doi.org/10.1016/j.ctrv.2017.11.002
Kudo M, Finn RS, Qin S, Han KH, Ikeda K, Piscaglia F, Cheng AL (2018) Lenvatinib versus sorafenib in first-line treatment of patients with unresectable hepatocellular carcinoma: a randomised phase 3 non-inferiority trial. Lancet 391:1163–1173. https://doi.org/10.1016/S0140-6736(18)30207-1
Li K, Xiao K, Zhu S, Wang Y, Wang W (2022) Chinese herbal medicine for primary liver cancer therapy: perspectives and challenges. Front Pharmacol 13:889799. https://doi.org/10.3389/fphar.2022.889799
Llovet JM, Montal R, Sia D, Finn RS (2018) Molecular therapies and precision medicine for hepatocellular carcinoma. Nat Rev Clin Oncol 15:599–616. https://doi.org/10.1038/s41571-018-0073-4
Llovet JM, Ricci S, Mazzaferro V, Hilgard P, Gane E, Blanc JF, Group SIS (2008) Sorafenib in advanced hepatocellular carcinoma. N Engl J Med 359:378-390. https://doi.org/10.1056/NEJMoa0708857
Ma S, Meng Z, Chen R, Guan KL (2019) The hippo pathway: biology and pathophysiology. Annu Rev Biochem 88:577–604. https://doi.org/10.1146/annurev-biochem-013118-111829
Nong J, Kang K, Shi Q, Zhu X, Tao Q, Chen YG (2021) Phase separation of Axin organizes the beta-catenin destruction complex. J Cell Biol 220:e202012112. https://doi.org/10.1083/jcb.202012112
Perugorria MJ, Olaizola P, Labiano I, Esparza-Baquer A, Marzioni M, Marin JJG, Banales JM (2019) Wnt-beta-catenin signalling in liver development, health and disease. Nat Rev Gastroenterol Hepatol 16:121–136. https://doi.org/10.1038/s41575-018-0075-9
Petrick JL, Florio AA, Znaor A, Ruggieri D, Laversanne M, Alvarez CS, McGlynn KA (2020) International trends in hepatocellular carcinoma incidence, 1978–2012. Int J Cancer 147:317–330. https://doi.org/10.1002/ijc.32723
Rao CV, Asch AS, Yamada HY (2017) Frequently mutated genes/pathways and genomic instability as prevention targets in liver cancer. Carcinogenesis 38:2–11. https://doi.org/10.1093/carcin/bgw118
Shariff MI, Cox IJ, Gomaa AI, Khan SA, Gedroyc W, Taylor-Robinson SD (2009) Hepatocellular carcinoma: current trends in worldwide epidemiology, risk factors, diagnosis and therapeutics. Expert Rev Gastroenterol Hepatol 3:353–367. https://doi.org/10.1586/egh.09.35
Singal AG, Lampertico P, Nahon P (2020) Epidemiology and surveillance for hepatocellular carcinoma: new trends. J Hepatol 72:250–261. https://doi.org/10.1016/j.jhep.2019.08.025
Villanueva A (2019) Hepatocellular carcinoma. N Engl J Med 380:1450–1462. https://doi.org/10.1056/NEJMra1713263
Wang S, Li H, Wang G, Zhang T, Fu B, Ma M, Chen G (2016) Yes-associated protein (YAP) expression is involved in epithelial-mesenchymal transition in hepatocellular carcinoma. Clin Transl Oncol 18:172–177. https://doi.org/10.1007/s12094-015-1353-4
Weiler SME, Lutz T, Bissinger M, Sticht C, Knaub M, Gretz N, Breuhahn K (2020) TAZ target gene ITGAV regulates invasion and feeds back positively on YAP and TAZ in liver cancer cells. Cancer Lett 473:164–175. https://doi.org/10.1016/j.canlet.2019.12.044
Weinberg RA (1995) The retinoblastoma protein and cell cycle control. Cell 81:323–330. https://doi.org/10.1016/0092-8674(95)90385-2
Wu H, Liu Y, Jiang XW, Li WF, Guo G, Gong JP, Ding X (2016) Clinicopathological and prognostic significance of Yes-associated protein expression in hepatocellular carcinoma and hepatic cholangiocarcinoma. Tumour Biol 37:13499–13508. https://doi.org/10.1007/s13277-016-5211-y
Yau T, Yao TJ, Chan P, Wong H, Pang R, Fan ST, Poon RT (2011) The significance of early alpha-fetoprotein level changes in predicting clinical and survival benefits in advanced hepatocellular carcinoma patients receiving sorafenib. Oncologist 16:1270–1279. https://doi.org/10.1634/theoncologist.2011-0105
Yu FX, Zhao B, Panupinthu N, Jewell JL, Lian I, Wang LH, Guan KL (2012) Regulation of the Hippo-YAP pathway by G-protein-coupled receptor signaling. Cell 150:780–791. https://doi.org/10.1016/j.cell.2012.06.037
Zhang Y, Wang X (2020) Targeting the Wnt/beta-catenin signaling pathway in cancer. J Hematol Oncol 13:165. https://doi.org/10.1186/s13045-020-00990-3
Zhao B, Li L, Lei Q, Guan KL (2010) The Hippo-YAP pathway in organ size control and tumorigenesis: an updated version. Genes Dev 24:862–874. https://doi.org/10.1101/gad.1909210